Probing Intermolecular Forces and Potentials with Magnetic Feedback Chemical Force Microscopy

Paul D. Ashby, Liwei Chen, and Charles M. Lieber*

Contribution from the Department of Chemistry and Chemical Biology, Harvard University, Cambridge, Massachusetts 02138

Received June 9, 2000. Revised Manuscript Received August 7, 2000

Abstract: Magnetic feedback chemical force microscopy (MF-CFM) was used to map the complete force profile between hydroxyl- and carboxyl-terminated self-assembled monolayers (SAMs) in aqueous solution. The snap-to-contact and snap-out instabilities intrinsic to force-displacement measurements made with weak spring constant cantilevers were eliminated by using a cantilever with an attached magnetic particle and a solenoid in a servo loop to balance the tip−sample interactions. The interaction between hydroxyl-terminated surfaces in deionized water was well fit by a van der Waals model to short distances. The Hamaker constant that was determined from experiment, 1.0×10^{-19} J, is similar to that expected for a gold−gold interaction and shows that the underlying gold support dominates the attractive interaction over a large range of separations. The interaction between a carboxyl-terminated tip and a sample in 0.010 M phosphate buffer at pH 7.0 was fit with a model that includes both van der Waals and electrostatic terms. The Hamaker constant, 1.2×10^{-19} J, which is similar to that obtained for hydroxyl-terminated surfaces, confirms that the gold−gold interaction dominates the attractive part of the interaction. In addition, the Debye length, 2.9 nm, surface potential, -1.5×10^2 mV, and charge regulation parameter, −0.71, obtained from analysis of the data are consistent with previous work (Vezenov et al. *J. Am. Chem. Soc.* **1997**, *119*, 2006−2015. Hu; Bard. *Langmuir* **1997**, *13*, 5114−5119). The implications of these results and applications of MF-CFM are discussed.

Introduction

The atomic force microscope (AFM)[1] is a very powerful tool for exploring the nanoscale world. Although it was originally developed as a qualitative imaging apparatus, within recent years, AFM has been used for measuring mechanical and electric properties, adhesion forces, and other quantitative applications.[2−5] The AFM can, with high sensitivity and spatial resolution, probe forces between a tip and a sample in solution, and thus can provide information that is critical to understanding potential energy surfaces through the measurement of force profiles. A force profile is the derivative of a one-dimensional projection of the potential energy surface in which the reaction coordinate is defined by the pulling direction. The potential energy surface, which determines both the energetics and the dynamics of the reaction, can then be reconstructed by integration. Unfortunately, in most AFM experiments there exists a region in the potential energy surface where the derivative of the force profile (second derivative of the potential energy surface) exceeds the stiffness of the AFM cantilever (Figure 1a). This condition causes the tip to snap to contact during approach and snap out during separation,[4] thus precluding measurement of the attractive portion of the potential at small separations. In supramolecular systems such as molecular recognition and protein folding, in which the potential energy surface is very rugged, this drawback

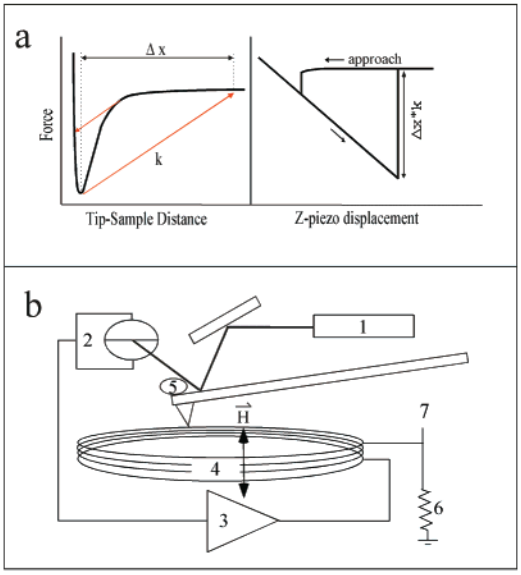

Figure 1. (a) Schematic representations of force profile (left) and measured force vs Z-piezo displacement (right). The red arrows indicate the trajectory of the cantilever in the region where the gradient in the profile exceeds the fixed spring constant, *k*, of the cantilever, leading to snap-in and snap-out. (b) The magnetic feedback (MF) schematic representation, where numbers 1−7 correspond to the laser diode, split photodiode, variable gain amplifier, solenoid, SmCo magnet, current sensing resistor, and controller, respectively.

* To whom correspondence should be addressed.

(1) Binnig, G.; Quate, C. F.; Gerber, C. *Phys. Rev. Lett.* **1986**, *56*, 930−933.

(2) Hamers, R. J. *J. Phys. Chem.* **1996**, *100*, 13103−13120.

(3) (a) Bustamante, C.; Rivetti, C.; Keller, D. J. *Curr. Opin. Struct. Biol.* **1997**, *7*, 709−716. (b) Kasas, S.; Thomson, N. H.; Smith, B. L.; Hansma, P. K.; Miklossy, J.; Hansma, H. G. *Int. J. Imaging Syst. Technol.* **1997**, *8*, 151−161.

(4) Noy, A.; Vezenov, D. V.; Lieber, C. M. *Annu. Rev. Mater. Sci.* **1997**, *27*, 381−421.

(5) (a) Carpick, R. W.; Salmeron, M. *Chem. Rev.* **1997**, *97*, 1163−1194. (b) Gewirth, A. A.; Niece, B. K. *Chem. Rev.* **1997**, *97*, 1129−1162. (c) Takano, H.; Kenseth, J. R.; Wong, S. S.; O'Brien, J. C.; Porter, M. D. *Chem. Rev.* **1999**, *99*, 2845−2890.

10.1021/ja0020613 CCC: $19.00 © 2000 American Chemical Society
Published on Web 09/14/2000

of conventional AFM leads to the loss of crucial information. The potential energy surface can be reconstructed using indirect methods such as measuring the anharmonicity of a tapping cantilever[6] or the Brownian motion of an undriven cantilever.[7] However, a very stiff cantilever is required to measure the whole force profile directly.

Two schemes to control the effective stiffness of the cantilever and, thus, eliminate mechanical instabilities have been reported.[8−12] First, interfacial force microscopy (IFM),[8] which is based on a differential-capacitance sensor and a force feedback system, electrostatically stiffens the cantilever. IFM has been used to measure force profiles between SAM-modified substrates and probes in air.[9] Unfortunately, this electrostatic technique cannot be used in high-ionic-strength solution because the electrostatic screening by ions in solution reduces the usable distance over which the feedback is effective. In addition, polarizable samples could be perturbed by the electric fields used for controlling cantilever stiffness. The second approach uses magnetic feedback to stiffen the cantilever[10] and has been utilized to measure force profiles in ultrahigh vacuum and air.[11,12] These initial studies have not, however, investigated the applicability of magnetic feedback to measure interactions between chemically well-defined surfaces in the condensed phase. In this paper, the power and versatility of using magnetic feedback to study intermolecular forces and potentials between chemically well-defined surfaces is shown by mapping the force profiles between hydroxyl- and carboxyl-terminated self-assembled monolayers (SAMs) in aqueous solution.

Experimental Section

Magnetic Tip Preparation. An inverted optical microscope equipped with micromanipulators was used to prepare the magnetic tips by gluing small SmCo magnets onto triangular Si_3N_4 (NP probes, $k = 0.06-0.6$ N/m, Digital Instruments, Inc., Santa Barbara, CA) cantilevers using UV curable adhesive. The small magnets (5−20μm in diameter) were prepared by crushing a larger SmCo magnet (CR54−314, Edmond Scientific, Inc., Barrington, NJ), spreading the resulting powder on a plastic film, and stretching the film to separate small pieces. The inverted microscope (Epiphot 200, Nikon, Excel Technologies, Enfield, CT) was equipped with three micromanipulators (461-XYZ-M, Newport, Irvine, CA), which were used to manipulate the Si_3N_4 cantilever, a sharpened tungsten wire probe, and the plastic film with magnet fragments. A small magnet fragment was attached to the cantilever using the following sequence: (i) the tungsten wire probe, which was dipped in glue (optical adhesive no. 63, Norland Products, New Brunswick, NJ), was used to deposit a small patch of glue on the backside of the cantilever; (ii) the wire was used to pick up a single magnet fragment from the plastic film and deposit this on the back of the cantilever; and (iii) the glue was cured for at least 1 h using an UV lamp (UVGL-25 mineralight lamp, UVP Inc., San Gabriel, CA).

Chemical Surface Preparation. The chemically well-defined surfaces were prepared by making SAMs from organic thiols. Gold layers were prepared on the magnetic tips using a thermal evaporator to slowly (1 Å/s) deposit a 70-nm layer of Au on a 7-nm Cr adhesion layer. Flat gold substrate surfaces 20 nm in thickness were deposited at 1.5 Å/s on freshly cleaved mica by electron beam evaporation at a substrate temperature of 350 °C. The evaporation pressures were typically 5×10^{-7} and 7×10^{-7} Torr for the thermal and the electron beam evaporators, respectively.

The SAM layers were made by immersing tips and samples in 400 μM ethanol solutions of either 11-mercaptoundecanol or 16-mercaptohexadecanoic acid for 1−2 hours[13] before rinsing with ethanol and drying under a stream of nitrogen. The measurements on hydroxyl-terminated SAM tip and sample surfaces were performed in deionized water, and the experiments using carboxyl-terminated SAM tip and sample surfaces were carried out in 0.010 M phosphate buffer, pH 7.0.

Magnetic Feedback. A schematic representation of the magnetic feedback system used in our experiments is shown in Figure 1b. The setup implements a servo loop, which includes an optical beam deflection detector of the cantilever position, a variable gain amplifier, a solenoid, and a cantilever with attached magnetic particle to balance the tip−sample interaction. A Digital Instruments Multimode AFM, equipped with a signal-access module between the microscope and the phase extender, was used unmodified. The cantilever deflection, measured by the AFM photodiode difference voltage was obtained from the signal access module and was smoothed by a single-pole low-pass filter before it was input into the amplifier. The cutoff frequency of the low-pass filter was chosen such that the loop gain reached unity before phase shifts, from feedback electronics and the cantilever resonance, total 180° and cause oscillations. The filtered signal was amplified by a power op amp (PA10, Apex Microtechnologies, Tucson, AZ) configured as a variable inverting amplifier, which was used to drive a solenoid and a small current sensing resistor. The solenoid was 400 turns of 32-gauge wire wrapped around a hollow aluminum spindle with an inner diameter of 1.5 mm and height of 5 mm. The AFM sample disk and mica sample were glued to opposite sides of the spindle so that the whole sample assembly mounted securely on top of the scanner (D scanner, Digital Instruments, Inc., Santa Barbara, CA) that was used for the experiments. The current-sensing resistor had a value of ∼10 Ω, and the output voltage was input into the Nanoscope III controller using an auxiliary data channel. The gradient in the magnetic field produced by the solenoid places a force on the magnetic particle, restoring the deflection and closing the feedback loop while the sample is moved in and out of contact with the tip.

Data Collection. Force curves, force vs z-piezo displacement, were acquired by recording both the cantilever deflection and the solenoid current while the sample surface was moved in and out of contact with the tip. Each curve contained 512 points over a scan range of 20 nm for hydroxyl−hydroxyl interaction data and over 75 nm for carboxyl−carboxyl interaction data. Piezo extension (tip−sample approach) and retraction (tip−sample separation) were done at a rate of 0.5−1 Hz. Typically, sets of fifty cycles were saved with the feedback on and the feedback off.

Tip and Feedback Calibration. Calibration of the cantilever was completed after force curves were acquired. With magnetic feedback off, the sensitivity (nm/V_c) of the cantilever deflection detection system was determined from the region of the force curve dominated by cantilever compliance. The open-loop gain and sensitivity of the magnetic feedback were calibrated by the input of a low-frequency square wave (∼2 Hz) into the low-pass filter. The input wave, solenoid current, and cantilever deflection were recorded. The solenoid current was measured as a voltage (V_s) at the current-sensing resistor. Using the solenoid voltage (V_s), cantilever deflection (V_c), sensitivity (nm/V_c), and spring constant (N/m), the force sensitivity of the system (N/V_s) could be determined. Multiple input voltages were used to ensure linearity. The thermal noise spectrum in air was used to calibrate the spring constant of each cantilever.[14] The spring constants of 0.69 N/m and 0.092 N/m were determined for the cantilevers that contained hydroxyl- and carboxyl-terminated SAMs, respectively.

(6) (a) O'Shea, S. J.; Welland, M. E. *Langmuir* **1998**, *14*, 4189−4197. (b) Gotsmann, B.; Anczykowski, B.; Seidel, C.; Fuchs, H. *Appl. Surf. Sci.* **1999**, *140*, 314−319. (c) Holscher, H.; Allers, W.; Schwartz, U. D.; Schwarz, A.; Wiesendanger, R. *Phys. Rev. Lett.* **1999**, *83*, 4780−4783.

(7) (a) Cleveland, J. P.; Schaffer, T. E.; Hansma, P. K. *Phys. Rev. B* **1995**, *52*, R8692−R8695. (b) Willemsen, O. H.; Kuipers, L.; van der Werf, K. O.; de Grooth, B. G.; Greve, J. *Langmuir* **2000**, *16*, 4339−4347. (c) Heinz, W. F.; Antonik, M. D.; Hoh, J. H. *J. Phys. Chem. B* **2000**, *104*, 622−626.

(8) Joyce, S. A.; Houston, J. E. *Rev. Sci. Instrum.* **1991**, *62*, 710−715.

(9) Thomas, R. C.; Houston, J. E.; Crooks, R. M.; Kim, T.; Michalske, T. A. *J. Am. Chem. Soc.* **1995**, *117*, 3820−3834.

(10) Jarvis, S. P.; Dürig, U.; Lantz, M. A.; Yamada, H.; Tokumoto, H. *Appl. Phys. A* **1998**, *66*, S211−S213.

(11) Yamamoto, S.-I.; Yamada, H.; Tokumoto, H. *Rev. Sci. Instrum.* **1997**, *68*, 4132−4136.

(12) Jarvis, S. P.; Yamada, H.; Yamamoto, S.-I.; Tokumoto, H.; Pethica, J. B. *Nature* **1996**, *384*, 247−249.

(13) Bain, C. D., Troughton, E. B., Tao, Y.-T., Whitesides, G. M., Nuzzo, R. G. *J. Am. Chem. Soc.* **1989**, *111*, 321−335.

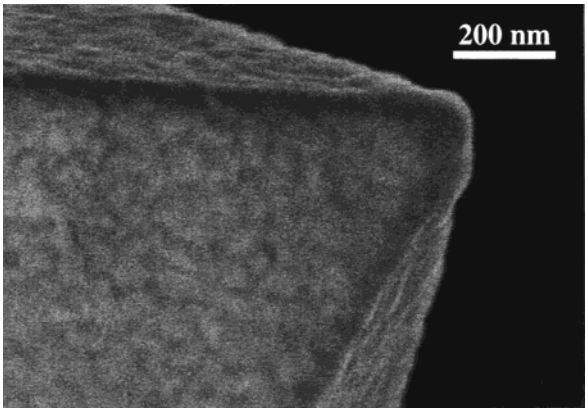

Figure 2. SEM image of the tip of the cantilever used in MF-CFM measurements of the carboxyl-functionalized surfaces.

A scanning electron microscope (SEM) image of the apex of a carboxyl-terminated SAM tip is shown in Figure 2. The image is representative of the tips used for MF-CFM experiments and was taken after the tip was used for collecting data. The gold grain at the apex defines the radius of curvature of the tip. The tip radii were calculated from SEM images using Igor Pro (Wavemetrics Inc., Lake Oswego, OR); specifically, the coordinates of three points on the edge of the apex were used to define a circle having the radius that was used for data analysis. The radii of curvature were 75 and 70 nm for the hydroxyl- and carboxyl-fuctionalized tips, respectively.

Data Analysis. The force profiles used for model fitting are an average of 6−17 curves. The raw data were imported into Igor Pro and scaled for force and z-piezo displacement as follows. The portion of the curves corresponding to large tip−sample separation (no interaction) is used to define zero force. The force contributions from deflection and solenoid current were summed and plotted against a tip−sample distance scale that was adjusted for the cantilever deflection. The movement of the cantilever caused the tip−sample spacing between the data points to be irregular. An interpolation algorithm was used to reconstruct the curve with even spacing. To adjust for drift, the z-piezo displacement scale of the hydroxyl−hydroxyl interaction data was shifted such that all curves overlapped at zero force in the contact region. The carboxyl−carboxyl data was similarly shifted such that the curves overlapped in the van der Waals attractive region. The hydroxyl−hydroxyl approach data was fit with a model for van der Waals interaction, and the carboxyl−carboxyl force profile was fit with a model that included attractive van der Waals and repulsive electrostatic terms (details below).

Results and Discussion

Magnetic Feedback. Magnetic feedback is effective in removing the instability associated with force profile measurements with soft springs. At short distances, a shallow barrier separates the well of the tip−sample potential and the spring well when the cantilever and force profile have similar stiffness. Thermal fluctuations are enough to overcome the barrier, and the system will snap from one well to the other or show bistability. A characteristic approach curve with magnetic feedback off for hydroxyl-terminated SAMs on the tip and sample surfaces is displayed in Figure 3a. The instability in the force profile is evident as the tip snaps to contact with the sample when it enters the steep region of the potential surface. To map continuously, the force profile requires that the cantilever stiffness be greater than the steepest gradient in the force profile. The magnetic feedback enables us to increase the stiffness and to achieve this goal. Specifically, Figure 3b,c shows the force contributions from the intrinsic stiffness of the cantilever and the magnetic feedback, respectively, for the same hydroxyl-terminated tip−sample used to record Figure 3a. These data demonstrate several important points. First, the data show clearly that the magnetic feedback has eliminated the mechanical instability (snap-in) during approach. Similarly, the instability during separation (snap-out) was also eliminated with the magnetic feedback. Second, the deflection of the cantilever was greatly reduced during approach such that its contribution to the restoring force measured only 75 pN (Figure 3b), while the magnetic feedback contributed most of the restoring force of 750 pN (Figure 3c).

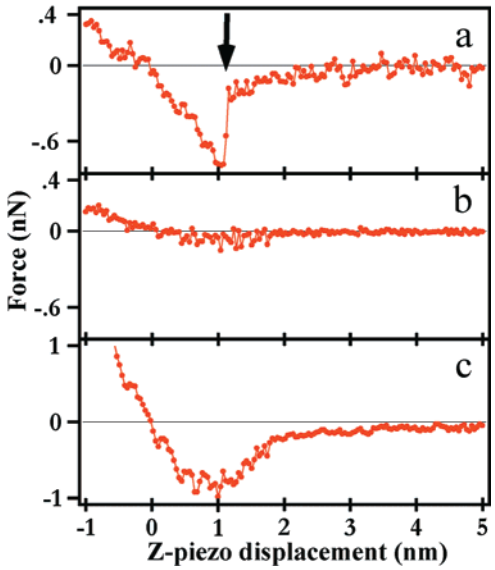

Figure 3. Data traces of hydroxyl-terminated SAM surfaces in solution during approach. (a) Deflection trace (displayed as force) without magnetic feedback has the characteristic snap-in indicated by the arrow. (b) Deflection trace (displayed as force) with magnetic feedback has no instabilities and a reduced total deflection. (c) Force due to magnetic feedback.

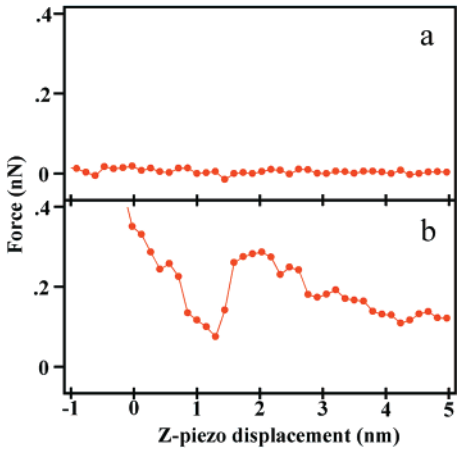

Figure 4. Data traces of carboxyl-terminated SAM surfaces in solution during approach. (a) Deflection trace (displayed as force) with magnetic feedback has no instabilities. (b) Force due to magnetic feedback system reveals the major features in the force profile.

The utility of MF-CFM was further demonstrated in studies of carboxyl-terminated SAM modified tips and samples. In this case, a much softer cantilever was used than for the hydroxyl-terminated SAM surfaces, 0.092 N/m vs 0.69 N/m, respectively. Significantly, Figure 4 shows that the magnetic feedback enables complete control of the cantilever during approach, even though the attractive part of the carboxyl−carboxyl interaction has a stiffness of ca. 0.9 N/m, which is ten times that of the cantilever. In these magnetic feedback experiments, the deflection of the

(14) Hutter, J. L.; Bechhoefer, J. *Rev. Sci. Instrum.* **1993**, *64*, 1868−1873.

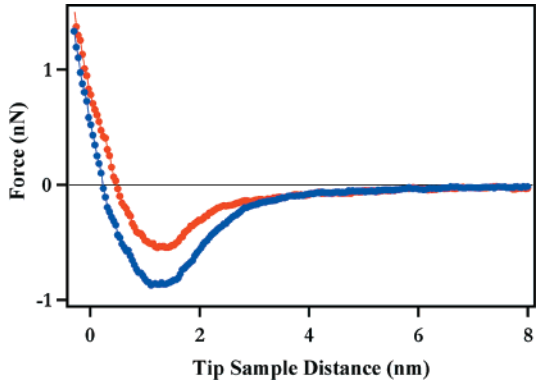

Figure 5. Approach (red) and separation (blue) force profiles for the hydroxyl-terminated tip−sample interaction.

cantilever was again small, with the major force contribution from the magnetic feedback. For example, at the peak of the electrostatic repulsive region of the potential (ca. 2 nm separation), the intrinsic cantilever contribution (from deflection) was 5 pN force (Figure 4a), in contrast to the magnetic feedback's contribution of ca. 290 pN (Figure 4b). Magnetic feedback clearly provides the necessary effective spring constant to smoothly measure stiff force profiles, and thus broadens significantly the possibilities for quantitative interfacial potential measurements using CFM.

Approach-Separation Hysteresis. Force profiles for the hydroxyl−hydroxyl interaction during both tip−sample approach (red) and separation (blue) are shown in Figure 5. Some hysteresis exists between the approach and separation curves, as evidenced by a 0.3-nm difference at the point of zero force in the contact region. The total adhesion for the separation is 850 pN, which is ca. 300 pN greater than the adhesion determined from the approach curve. Adhesion hysteresis can be attributed to an inherent irreversibility associated with loading and unloading or bonding and unbonding of the SAM surfaces.[15] Hysteresis in the loading and unloading of a SAM surface has previously been studied using IFM.[16] The contact pressure in these previous experiments was greater than 3.0 GPa, and was suggested to produce a rearrangement of the SAM.[17] The maximum pressure in our MF-CFM experiments, 1.4 GPa,[18] is less than the pressure expected to rearrange substantially the SAM layer. Hence, we believe that the hysteresis is caused by small molecular rearrangements of the SAM terminal groups to facilitate interfacial bonding and elastic deformation of the underlying gold support. This same principle is responsible for the discrepancy in advancing and receding values for contact angle measurements.[19]

The minimum of the MF-CFM separation force profile is a measure of the total adhesion. A histogram of the total adhesion for the hydroxyl surfaces data is grouped around a value of 1100 pN, with a standard deviation of 400 pN. In measurements with magnetic feedback off, a histogram of the snap-out adhesion is grouped around 800 pN, with a standard deviation of 300 pN. The higher effective spring constant of the cantilever with magnetic feedback on leads to a larger total applied force because the piezo movement in the contact region is constant between the experiments. We believe that this larger applied force leads to more rearrangement and elastic deformation at the interface and, thus, can explain the discrepancy between the histograms. Because of this rearrangement of the surface upon loading, we believe that the approach force profiles will provide a better measure of the intrinsic potential surface.

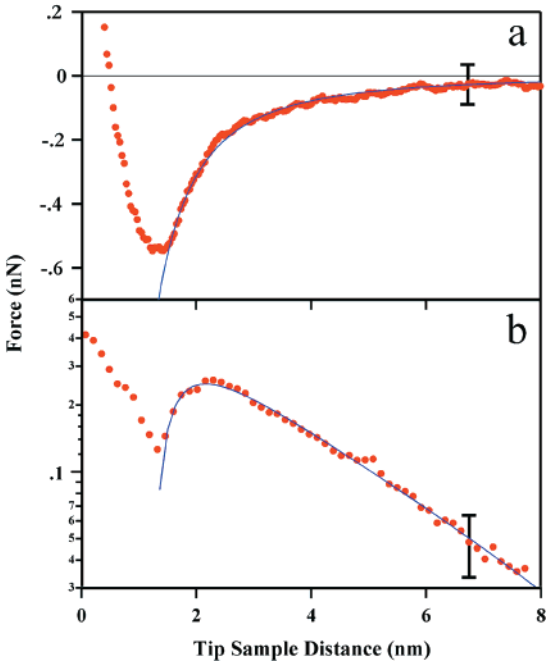

Figure 6. Force profiles for (a) hydroxyl-terminated SAMs in deionized water and (b) carboxyl-terminated SAMs in 0.010 M, pH 7 phosphate buffer. Both profiles were recorded while approaching the sample to the tip. Experimental data are red solid circles and fits are solid blue lines. The error bars in (a) and (b) are representative of the respective data sets.

van der Waals Interaction. We have used the MF-CFM data acquired on approach to analyze the interaction between the hydroxyl-terminated and the carboxyl-terminated tip and sample surfaces. The complete approach force profile for the hydroxyl−hydroxyl interaction is shown in Figure 6a. The long-range attractive region of the force profile was fit by an inverse square power law[20] (blue line) expected for the van der Waals interaction between a sphere and a flat surface.[21] The parameters used in the fit were the Hamaker constant and a tip−sample distance offset.

The value of the Hamaker constant obtained from fits to our force profiles for the hydroxyl-terminated SAM surfaces was 1.0×10^{-19} J. Comparison of this value to the reported Hamaker constants for alkanes interacting through water and gold surfaces in water, 4×10^{-21} J[15] and 1×10^{-19} J,[22] respectively, shows

(15) Isaelachvili, J. *Intermolecular and Surface Forces,* 2nd ed.; Academic Press: San Diego, 1992.

(16) Joyce, S. A.; Thomas, R. C.; Houston, J. E.; Michalske, T. A.; Crooks, R. M. *Phys. Rev. Lett.* **1992**, *68*, 2790−2793.

(17) Tupper, K. J.; Brenner, D. W. *Langmuir* **1994**, *10*, 2335.

(18) For a sphere interacting with a flat surface, the maximum pressure, P_{max}, can be estimated using the JKR model:[15]

$$P_{\max} = \frac{3Ka}{2\pi R} - \left(\frac{3KW_{12}}{2\pi a}\right)^{1/2}$$

where a is the contact radius, R is the radius of curvature of the tip, K is the Young modulus, and W_{12} is the surface energy. For a 75-nm radius of curvature tip (typical of those used in our experiments) and a maximum applied load of 25 nN, the maximum pressure is 1.4 GPa.

(19) Israelachvili, J.; Berman, A. *Isr. J. Chem.* **1995**, *35*, 85−91.

(20) The inverse square power law:

$$F = -\frac{AR}{6(D - D_0)^2}$$

where A is the Hamaker constant, R is the tip radius, D is the relative tip−sample distance and D_o is an offset parameter with respect to the absolute zero of tip−sample separation.

(21) Integration of the familiar $F = 1/r^7$ ($W = 1/r^6$) interaction for point particles produces a $1/r^2$ power law.[15]

(22) Kane, V.; Mulvaney, P. *Langmuir* **1998**, *14*, 3303−3311.

that our results are the same as the value for gold surfaces interacting through water. Our Hamaker constant is also consistent with the range of values, $0.9-3 \times 10^{-19}$ J, computed from the most reliable spectroscopic data for gold surfaces.[23,24] These comparisons suggest strongly that the gold support dominates the long-range attractive interaction in the Au−SAM system. The hydroxyl-terminated SAM is approximately 1.3 nm thick.[25] This thin SAM layer has a much smaller polarizability than the underlying gold, and thus, the SAM only becomes the dominate contributor to the forces at distances of less than 0.3 nm before contact.[26] The absolute tip−sample distance was also determined from the fits. After analyzing the data, the tip−sample distance scale was shifted by the offset value, D_0. The MF-CFM data also extends to chemically relevant short-range attractive interactions and contact; however, no simple models exist which can treat these ensemble chemical interactions. We believe that control of the orientations of the interacting terminal groups will be required to understand these important short-range attractive interactions in detail.

van der Waals and Double-Layer Interactions. The physical and chemical properties of carboxyl-terminated SAM surfaces were also determined using MF-CFM. The approach force profile for the carboxyl−carboxyl interaction is shown in Figure 6b. The experiments were completed in 0.010 M phosphate buffer at pH 7.0 where the carboxyl-end groups on both surfaces are partially deprotonated.[27,28] At long range, the electrostatic repulsion between the two surfaces, due to charged carboxylate groups, dominates the force profile. This repulsive regime has been observed with the surface forces apparatus and in previous AFM experiments and can be analyzed using a double-layer model.[15,27−29] Significantly, the MF-CFM data show that at small separations, the steep attractive van der Waals contribution to the overall interaction also can be reliably mapped.

To analyze our complete force profiles, we used a model that includes a repulsive electrostatic term and an attractive van der Waals term.[30] The fit (blue line) to the data in Figure 6b was excellent with good agreement through the regime of electrostatic repulsion and into the attractive region due to the van der Waals interaction. The parameters of the fit were the Hamaker constant, surface potential, Debye length, charge regulation parameter, and the tip−sample distance offset. Notably, we found only a single self-consistent solution for the parameters that were used to fit the data. The Hamaker constant, 1.2×10^{-19} J, from the van der Waals term, confirmed that the gold−gold interaction dominates the long-range van der Waals interaction in these Au−SAM systems. The similarity of the hydroxyl and carboxyl values and their agreement with theory and past experiment confirmed the accuracy of MF-CFM for potential measurements.

We have analyzed the parameters due to the electrostatic interactions and compared these to previous studies[27,28,31−34] because this repulsive regime can be measured without magnetic feedback. The results from our fit for the electrostatic terms are Debye length, 2.9 nm; surface potential, -1.5×10^2 mV; and charge regulation parameter, -0.71.[35,36] The surface potential value from these new experiments, -1.5×10^2 mV, is consistent with previous work in this lab.[27] The surface charge density obtained from the potential, -0.12 C/m^2,[2,35,37] indicated that the surface was 15.3% ionized at pH 7 and that the surface pK_a was 7.7. This slightly elevated value is consistent with previous work.[27,28,31−34] The charge regulation parameter, -0.71, strongly implied that the carboxyl surface exhibits constant charge behavior during approach. This conclusion is also consistent with previous experiments carried out in our lab[27] and by Hu and Bard.[28]

Conclusions

This work used MF-CFM to map the force profiles between chemically well-defined surfaces in solution. The magnetic feedback removes cantilever instabilities so that important intermolecular interactions can be fully characterized. Studies of hydroxyl-terminated and carboxyl-terminated SAM modified tips and samples have shown clearly that the underlying gold−gold van der Waals interaction dominates the attractive part of the interaction down to relatively short distances with a Hamaker constant of 1×10^{-19} J. The complete force profiles obtained on the carboxyl-terminated SAMs also allow the surface potential, charge regulation parameter, and Debye length to be robustly determined, and moreover, to yield a pK_a of 7.7 in 0.010 M phosphate buffer.

(23) Parsegian, V. A.; Weiss, G. H. *J. Colloid Interface Sci.* **1981**, *81*, 285−289.

(24) Schrader, M. E. *J. Colloid Interface Sci.* **1984**, *100*, 372−380.

(25) Harder, P.; Grunze, M.; Dahint, R.; Whitesides, G. M.; Laibinis, P. E. *J. Phys. Chem. B* **1998**, *102*, 426−436.

(26) For a symmetric system with adsorbed layers on the substrate, the model for the force is

$$F(D) = \frac{R}{6}\left[\frac{A_{232}}{D^2} - \frac{2A_{123}}{(D+T)^2} + \frac{A_{121}}{(D+2T)^2}\right]$$

where R is the tip radius, T is the thickness of the adsorbed films, and D is the distance between the adsorbed layers.[15] A_{232} is the Hamaker constant for the adsorbed layers interacting through the medium, A_{123} is the Hamaker constant for the substrate and medium interacting through the adsorbed layer, and A_{121} is the Hamaker constant for the substrates interacting through the adsorbed layers. When the distance is much smaller than T, the equation reduces to $F(D) = RA_{232}/6D^2$. At larger distances, the full expression can be simplified to $F(D) = RA_{131}/6D^2$. In our experiments, the Hamaker constant for the gold−water−gold interaction, $A_{131} = 1 \times 10^{-19}$ J, is 2 orders of magnitude larger than the Hamaker constant for alkane−water−alkane, $A_{232} = 4 \times 10^{-21}$ J. With a SAM thickness of 1.3 nm, the van der Waals contribution from the SAM layer is small until separations are reduced to 0.3 nm or less.

(27) Vezenov, D. V.; Noy, A.; Rozsnyai, L. F.; Lieber, C. M. *J. Am. Chem. Soc.* **1997**, *119*, 2006−2015.

(28) Hu, K.; Bard, A. J. *Langmuir* **1997**, *13*, 5114−5119.

(29) Zhmud, B. V.; Meurk, A.; Bergstrom, L. *J. Colloid Interface Sci.* **1998**, *207*, 332−343.

(30) The DLVO model that includes linearized surface charge-potential regulation:[15]

$$F = \frac{2\epsilon\epsilon_0\Psi_0^2}{\lambda}\frac{e^{-(D-D_0-3.4)/\lambda}}{1+ae^{-(D-D_0-3.4)/\lambda}} - \frac{AR}{6(D-D_0)}$$

where Ψ_0 is the surface potential; ϵ, the dielectric constant; ϵ_0, the permittivity of space; λ, the Debye length; a, the charge regulation parameter; and A, D, and D_0 have the same meaning as in ref 20.

(31) White, H. S.; Peterson, J. D.; Cui, Q.; Stevenson, K. J. *J. Phys. Chem B* **1998**, *102*, 2930−2934.

(32) Creager, S. E.; Clarke, J. *Langmuir* **1994** *10*, 3675−3683.

(33) Smalley, J. F.; Chalfant, K.; Feldberg, S. W.; Nahir, T. M.; Bowden, E. F. *J. Phys. Chem. B* **1999**, *103*, 1676−1685.

(34) Wang, J.; Frostman, L. M.; Ward, M. D. *J. Phys. Chem.* **1992**, *96*, 5224−5228.

(35) The Debye length for this system is slightly longer than the 2.3 nm value calculated from the charge and concentration of the ions in the solution. Our value measured with magnetic feedback, 2.9 nm, is very similar to that obtained in a separate experiment without magnetic feedback, 3.1 nm, using freshly prepared 0.010 M phosphate buffer. We do not believe the deviation corresponds to a systematic error of MF-CFM.

(36) The relationship between surface charge and surface potential is $\sigma^2 = 2\epsilon\epsilon_0 kT(\sum_i \rho_{0i} - \sum_i \rho_{\infty i})$ and $\rho_{0i} = \rho_{\infty i}e^{-z_i e\psi_0/kT}$, where σ is the surface charge density, ϵ is the dielectric constant, ϵ_0 is the permittivity of space, k is Boltzmann's constant, T is temperature, $\rho_{\infty i}$ is the concentration of each ionic species in the bulk, z_i is the charge of the species, e is the electronic charge, and Ψ_0 is the surface potential. Using the measured surface potential of -1.5×10^2 mV and the concentrations of our buffer solutions ($[Na^+] = 0.01381$, $[H_2PO_4^-] = 0.00619$, $[HPO_4^{-2}] = 0.00381$) a surface charge of -0.12 C/m^2 was calculated.

(37) Strong, L.; Whitesides, G. M. *Langmuir* **1988**, *4*, 546−558.

A limitation of the present experiments is that the chemically important short-range interactions, although measured, cannot be analyzed in detail due to the tip. Specifically, conventional Si and Si_3N_4 probes, which have radii of 10−90 nm, preclude the possibility of defining the orientation of molecular interactions, and moreover, the underlying gold makes a large contribution to the force. These critical issues can be solved by using covalently functionalized carbon nanotube probes, which can be used to localize single molecular groups at the tip end[38,39] and thereby precisely to define the position and orientation of the interacting groups. MF-CFM experiments with nanotube tips should enable force profiles of complex systems along well-defined projections of the potential surface to be obtained, and such experiments could have a far-reaching impact on chemistry and biology.

Acknowledgment. We acknowledge helpful discussions with A. Noy, D. V. Vezenov, and J.-L. Huang. C.M.L. acknowledges support of this work by the Air Force Office of Scientific Research, and P.D.A. thanks the National Science Foundation for predoctoral fellowship support.

JA0020613

(38) (a) Wong, S. S.; Joselevich, E.; Woolley, A. T.; Cheung, C. L.; Lieber, C. M. *Nature* **1998**, *394*, 52−55. (b) Wong, S. S.; Woolley, A. T.; Joselevich, E.; Cheung, C. L.; Lieber, C. M. *J. Am. Chem. Soc.* **1998**, *120*, 8557−8558.

(39) (a) Hafner, J. H.; Cheung, C. L.; Lieber, C. M. *Nature* **1999**, *398*, 761−761. (b) Hafner, J. H.; Cheung, C. L.; Lieber, C. M. *J. Am. Chem. Soc.* **1999**, *121*, 9750−9751. (c) Cheung, C. L.; Hafner, J. H.; Lieber, C. M. *Proc. Natl. Acad. Sci. U.S.A.* **2000**, *97*, 3809−3813. (d) Cheung, C. L.; Hafner, J. H.; Odom, T. W.; Kim, K.; Lieber, C. M. *Appl. Phys. Lett.* **2000**, *76*, 3136−3138.